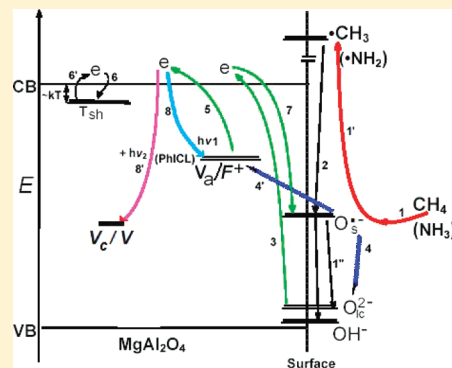


Photoinduced Radical Processes on the Spinel ( $\text{MgAl}_2\text{O}_4$ ) Surface Involving Methane, Ammonia, and Methane/AmmoniaA. V. Emeline,<sup>\*,†</sup> D. A. Abramkin,<sup>†</sup> I. S. Zonov,<sup>†</sup> N. V. Sheremetyeva,<sup>†</sup> A. V. Rudakova,<sup>†</sup> V. K. Ryabchuk,<sup>†</sup> and N. Serpone<sup>\*,‡</sup><sup>†</sup>Faculty of Physics, Saint-Petersburg State University, Saint-Petersburg, Russian Federation<sup>‡</sup>Gruppo Fotochimico, Dipartimento di Chimica, Università di Pavia, via Taramelli 10, Pavia, 27100 Italia

## Supporting Information

**ABSTRACT:** The present study explored photoinduced radical processes caused by interaction of  $\text{CH}_4$  and  $\text{NH}_3$  with a photoexcited surface of a complex metal oxide: magnesium–aluminum spinel ( $\text{MgAl}_2\text{O}_4$ ; MAS). UV irradiation of MAS *in vacuo* yielded V-type color centers as evidenced by the 360 nm band in difference diffuse reflectance spectra. Interaction of these H-bearing molecules with photogenerated surface-active hole states ( $\text{O}_5^-\bullet$ ) yielded radical species which on recombination produced more complex molecules (including heteroatomic species) relative to the initial molecules. For the MAS/ $\text{CH}_4$  system, photoinduced dissociative adsorption of  $\text{CH}_4$  on surface-active hole centers produced  $\bullet\text{CH}_3$  radicals that recombined to yield  $\text{CH}_3\text{CH}_3$ . For MAS/ $\text{NH}_3$ , a similar dissociative adsorption process led to formation of  $\bullet\text{NH}_2$  radicals with formation of  $\text{NH}_2\text{NH}_2$  as an intermediate product; continued UV irradiation ultimately yielded  $\text{N}_2$ . For the mixed MAS/ $\text{CH}_4$ / $\text{NH}_3$  system, however, interaction of adsorbed  $\text{NH}_3$  and  $\text{CH}_4$  on the UV-activated surface of MAS yielded  $\bullet\text{NH}_2$  and  $\bullet\text{CH}_3$  radicals, respectively, which produced  $\text{CH}_3\text{—NH}_2$  followed by loss of the remaining hydrogens to form a surface-adsorbed cyanide,  $\text{CN}_s$ , species. Recombination of photochemically produced radicals released sufficient energy to re-excite the solid spinel, generating new surface-active sites and a flash luminescence (emission decay time at 520 nm,  $\tau \sim 6$  s for the MAS/ $\text{NH}_3$  case) referred to as the PhICL effect.



## 1. INTRODUCTION

The photoassisted generation of surface radical species and the consequent secondary radical-induced chemical reactions are one of the major pathways of photoprocesses in heterogeneous photochemistry and photocatalysis. Generally, photoinduced radicals are formed as intermediate products of either photocatalytic redox processes (such as photocatalytic water decomposition leading to formation of  $\bullet\text{OH}$  radicals as intermediate products) or noncatalytic processes of homolytic dissociative photoinduced adsorption (e.g., photoadsorption of  $\text{CH}_4$  resulting in the formation of  $\bullet\text{CH}_3$  radicals as intermediate products).<sup>1–5</sup> From this point of view, all other reactions involving photoinduced radicals can be considered as side-reactions. Thus, all photocatalytic oxidation processes of organic compounds in aqueous media caused by  $\bullet\text{OH}$ -radical attack are simply incomplete photocatalytic water decomposition due to secondary oxidation reactions of organic substrates. The same is true for incomplete photoinduced dissociative adsorption, e.g., the secondary reaction of two methyl radicals yields ethane,<sup>4,5</sup> rather than a complete dissociative adsorption of methane on the surface. As a rule, it is remarkable that the catalytic or noncatalytic nature of the side-reactions conforms to the catalytic or noncatalytic nature of the “main” process. Thus, incomplete photocatalytic water decomposition in the presence of organic compounds leads to photocatalytic oxidative processes of the organic substrate,

while the incomplete noncatalytic dissociative photoadsorption of methane, for example, results in either its noncatalytic conversion to ethane or its noncatalytic oxidation to carbon dioxide.<sup>5</sup>

Whether a photostimulated surface reaction is catalytic or not plays an important role in the character of bulk photophysical processes in the solid part of heterogeneous systems. As shown earlier,<sup>6</sup> noncatalytic processes significantly change the efficiency of photostimulated defect formation in solids. In addition, the direction of altering a defect formation process is strongly dependent on the type of noncatalytic reactions. For instance, a surface oxidation reaction leads to an increase in the number of electron defect states, whereas a surface reduction reaction results in the additional formation of defects with trapped holes. This connection provides a tool to distinguish between catalytic and noncatalytic processes by monitoring defect formation in solids by spectroscopic means.<sup>6</sup>

Being highly energetic species, photochemically produced radicals can release energy during radical recombination processes, sufficient for recurring electronic excitation of solids. In particular, such secondary excitation manifests itself as generation of new surface-active sites and as flash luminescence

Received: January 25, 2012

Revised: April 5, 2012

Published: April 12, 2012



referred to as photo-induced chemisorption luminescence, the so-called PhICL effect,<sup>7–10</sup> typically observed during the photoinduced dissociative postadsorption of H-bearing molecules such as H<sub>2</sub>, H<sub>2</sub>O, CH<sub>4</sub> (and, in general, hydrocarbons), and NH<sub>3</sub>.

Recombination of radical species can result in the synthesis of more complex molecules relative to initial reagent molecules: e.g., recombination of •CH<sub>3</sub> radicals and •NH<sub>2</sub> radicals formed from the interaction of CH<sub>4</sub> and NH<sub>3</sub> with a photoexcited metal oxide surface would yield ethane and hydrazine, respectively. Therefore, radical-induced secondary reactions represent an important pathway to form complex molecules, particularly in nature.<sup>11–13</sup>

Spinel, MgAl<sub>2</sub>O<sub>4</sub>, is a complex wide band gap insulator ( $E_{\text{bg}} = 7.5\text{--}9.0$  eV)<sup>14,15</sup> possessing a cubic crystal lattice and a spinel-type structure, space group *Fd3m*,<sup>16</sup> in which cation vacancies are the predominant type of *intrinsic* defects. In addition, synthetic spinels are partly inverted (up to ca. 20%), i.e., a fraction of the Mg<sup>2+</sup> cations occupy the positions of Al<sup>3+</sup> ions and in turn the Mg<sup>2+</sup> positions are occupied by Al<sup>3+</sup> cations.<sup>17</sup> Such defects serve as hole and electron traps, respectively. Stoichiometric deviation results in the formation of either anion or cation vacancies ( $V_{\text{a}}$  and  $V_{\text{c}}$ , respectively). The existence of Schottky-type defects is thought to be rather unlikely because of the density of anion packing. Several UV- and radiation-induced *F* and *V* color centers have been identified in MgAl<sub>2</sub>O<sub>4</sub>.<sup>17,18</sup>

Earlier, we established that (i) the MgAl<sub>2</sub>O<sub>4</sub> spinel is an efficient photosorbent for O<sub>2</sub>, H<sub>2</sub>, CO, and CH<sub>4</sub> molecules; (ii) UV irradiation of the spinel surface produces both short-lived ( $\tau \sim 10^{-3}$  s) and long-lived ( $\tau > 10^{-3}$  s) adsorption centers for H<sub>2</sub> and O<sub>2</sub>; (iii) the photosorption of these gases produces strongly bound species, removable from the surface by thermal treatment at 300–900 K; and (iv) that such species could react with hydrogen without additional activation at ambient temperature.<sup>9</sup> The specific photoadsorption capacities ( $\Theta$ ) of this spinel were  $\Theta_{\text{O}_2} = (2.3 \pm 0.6) \times 10^{12}$  molecules cm<sup>-2</sup> and  $\Theta_{\text{H}_2} = (1.1 \pm 0.3) \times 10^{12}$  molecules cm<sup>-2</sup>, i.e., about an order of magnitude greater than the photoadsorption capacities of TiO<sub>2</sub>, ZnO, and BeO,<sup>20</sup> but otherwise commensurate with the photoadsorption capacity of silica modified with TiO<sub>2</sub> nanoclusters.<sup>21</sup> A later study<sup>8</sup> examined the photostimulated adsorption of molecular O<sub>2</sub> and H<sub>2</sub>, and their influence on the photocoloration of MAS in which we established that O<sub>2</sub> is photosorbed on *F*<sup>o</sup> and *F*<sup>+</sup> centers, while H<sub>2</sub> is photosorbed dissociatively on *V*-type centers (i.e., O<sup>-</sup> holes located at cation vacancies or at {(Mg<sup>2+</sup>)<sub>Al</sub>} centers typical of partially reversed spinels). The red spectral limit of photoactivation of these photostimulated processes at the surface and in the bulk of MAS occurred at about 250 nm, corresponding to the photoexcitation of *F*<sup>o</sup>- and *F*<sup>+</sup>-type centers.<sup>8</sup>

In the present study, we explore the photoinduced radical processes caused by interaction of CH<sub>4</sub>, NH<sub>3</sub>, and CH<sub>4</sub>/NH<sub>3</sub> with the photoexcited surface of this spinel metal oxide, whose structure is more complex than the more typical metal oxides TiO<sub>2</sub> and ZnO.

## 2. EXPERIMENTAL SECTION

A powdered sample of MgAl<sub>2</sub>O<sub>4</sub> (high-purity grade suitable for optical materials) was obtained from the S.I. Vavilov State Optical Institute, Russia. The specific surface area of the sample was determined by the BET method with nitrogen gas: ca. 14 m<sup>2</sup> g<sup>-1</sup>. X-ray diffraction

structural methods confirmed that the sample contained only the spinel crystalline form.

Ubiquitous organic impurities and adsorbed molecules on the metal oxide specimen surface were removed by a thermal pretreatment at  $T = 900$  K in an oxygen atmosphere (pressure, 100 Pa) and *in vacuo* for a few days. Reproduction of the original state of the specimens between experiments was achieved by heating in oxygen for ca. 1 h. Experimental errors in kinetic measurements that may have been caused by the nonreproducibility of the original state of the MgAl<sub>2</sub>O<sub>4</sub> specimen is estimated at less than ~10%.

Powdered samples were contained in a quartz cell (path length, 5 mm; illuminated area, 6 cm<sup>2</sup>) connected to a high-vacuum setup that was equipped with an oil-free pump system. The ultimate gas pressure in the reaction cell was ca. 10<sup>-7</sup> Pa. The volume of the reactor was 50 cm<sup>3</sup>. A Pirani-type manometer was used to measure gas pressures during the kinetic studies. Monitoring of the gas composition and identification of thermodesorption products were performed using a mass spectrometer (model MX-7301; Russia). Thermodesorption studies were carried out in the linear heating regime at a rate of 0.25 K min<sup>-1</sup>. Irradiation of the solid specimens was carried out with a 120 W high pressure mercury lamp (DRK-120, MELZ, Russia). The light irradiance at wavelengths below 400 nm (6 mW cm<sup>-2</sup>) was measured through a water filter using a thermo-element (IOFI, Russia; sensitivity, 1.5 V W<sup>-1</sup>). The photon flow at wavelengths below 250 nm was about 10<sup>15</sup> photons cm<sup>-2</sup> s<sup>-1</sup>.

Diffuse reflectance spectra (DRS; BaSO<sub>4</sub> was the reference) were recorded with a Specord M-40 spectrophotometer (Karl Zeiss, Jena, Germany) equipped with an integrating sphere assembly and interfaced to a computer. In our experiments, the movable high-vacuum setup/quartz cell system was moved as a unit between the positions of irradiation and of thermal treatment of the specimen to the position for recording spectra; both were fixed with high precision in appropriate positions.

FTIR spectra of surface reaction products were recorded using the high-vacuum stainless steel cell applied for low-temperature measurements described elsewhere.<sup>20,21</sup> Pressure was measured with two Edwards Barocel 600 pressure gauges attached to the cell. One gauge, with an accuracy of 10<sup>-3</sup> Torr and an upper measurement limit of 10 Torr, was attached directly to the inner volume of the cell, whereas the range of the other gauge was 1–1000 Torr used to measure the pressure of the gas to be admitted from the dosing volume. Temperature of the samples was measured using a thermocouple inserted into the coolant compartment close to the sample holder. FTIR spectra of surface reaction products were recorded at a spectral resolution of 4 cm<sup>-1</sup> for a total of 128 scans using a Nicolet 710 spectrometer equipped with a cooled MCT detector.

As-received powders of spinel MgAl<sub>2</sub>O<sub>4</sub>, commercial MgO, and  $\gamma$ -Al<sub>2</sub>O<sub>3</sub> (Degussa) of high purity were pressed into a pellet with a thickness of about 0.1 mm. The pellet was placed in the stainless steel cell and treated at 823 K (spinel), 1023 K (MgO), and 873 K ( $\gamma$ -Al<sub>2</sub>O<sub>3</sub>) for about 1 h in an oxygen atmosphere and then *in vacuo* at pressures no lower than 10<sup>-5</sup> Torr.

HCN was prepared by the reaction of H<sub>2</sub>SO<sub>4</sub> with KCN in the preliminary outgassed vacuum system. The gases/vapors were purified by passing through a trap kept at 190 K or condensed at 77 K with subsequent removal of incondensable gases.

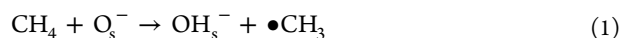
## 3. RESULTS AND DISCUSSION

**3.1. MAS/CH<sub>4</sub> System.** The mass spectrum of the product ethane that evolved into the gas phase during the photo-stimulated dissociative adsorption of methane on the UV-activated spinel surface is reported in Figure S1 (see Supporting Information).<sup>8,19</sup> The photosorption of methane also gave rise to the PhICL effect, whose emission spectrum corresponds to the emission spectra of photo- and thermo-stimulated luminescence of MAS.

The mechanism of the photostimulated dissociative adsorption of methane on metal oxide (e.g., TiO<sub>2</sub> and ZnO)

surfaces has been examined extensively in the past few decades.<sup>1–5</sup> Thus, the photosorption process is reasonably well understood.

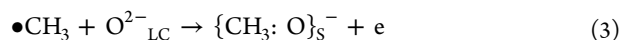
In the present instance, the first step of this process on spinel is interaction of methane with photoinduced surface-active hole centers,  $O_s^-$ , to yield methyl radicals (reaction 1):



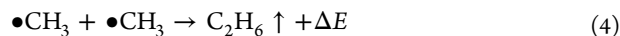
The subsequent step that completes the homolytic dissociative adsorption of methane is the interaction of the methyl radical with a surface electron active center,  $e_s$ , to form a surface adsorption complex,  $(CH_3:S)$ ; S denotes the metal oxide surface (reaction 2).



However, the appearance of methyl radicals on the surface initiates a set of various side reactions, such as, for example, interaction of the methyl radical with low-coordinated surface oxygen ions,  $O_{LC}^{2-}$ , leading to the formation of an adsorption complex,  $(CH_3:O)_s^-$ , and generation of free electrons (reaction 3).



Concomitantly, recombination of methyl radicals yields ethane that evolves into the gas phase and releases the bond energy commensurate with the formation of C–C bonds (reaction 4).



The bond energy ( $\Delta E$ ) so released is sufficient to re-excite the spinel to yield the excited state of the metal oxide. The free electron produced in reaction 3 is subsequently trapped by the solid's defects that results in emission of a photon. Either or both processes can lead simultaneously to the PhICL effect during the postadsorption of methane on the photoexcited surface of the solid, as observed in various wide band gap metal oxides.<sup>9,10</sup>

Clearly, formation of ethane occurs through recombination of the methyl radicals produced in eq 1. Recombination of photogenerated radicals has thus led to formation of a molecule more complex, in this particular instance, ethane, than the initial molecule methane.

**3.2. MAS/NH<sub>3</sub> System.** Historically, studies of photo-stimulated processes in gas–solid heterogeneous systems involving ammonia were, to the best of our knowledge, first reported in the early 1940s in a seminal article by Kasparov and Terenin,<sup>22</sup> who described the spectral dependencies of the photolysis of ammonia adsorbed on several metal oxide adsorbents, including alumina. These workers detected the evolution of a gaseous product that they believed to be hydrogen. Spectral dependencies of the photonic efficiency (i.e., photoactivity) in the UV spectral range were also reported.

Strong adsorption of ammonia (in the dark) is a characteristic feature of spinel ( $MgAl_2O_4$ ) and of several other metal oxides. Accordingly, in dealing with photostimulated processes in our experiments, the initial state of the heterogeneous system consisted of ammonia preadsorbed on the surface of MAS (average coverage, ca. 0.1 of a monolayer) at zero pressure in the gas phase. Surface processes related to photoinduced (postirradiation) effects were also investigated during the introduction of ammonia on the MAS surface preirradiated *in vacuo*.

UV irradiation of the MAS/preadsorbed NH<sub>3</sub> system led to the evolution of molecular nitrogen into the gas phase as the final product. Figure 1 illustrates the time evolution of the rate

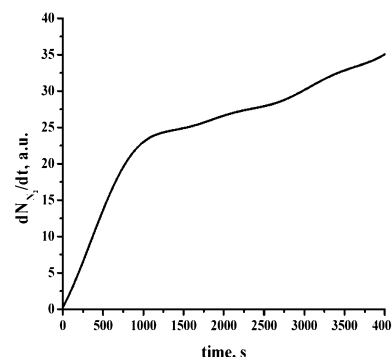


**Figure 1.** Time evolution of the rate of nitrogen release from the MAS surface during the photolysis of ammonia.

of nitrogen release from the MAS surface. An intermediate product (hydrazine) also formed on the surface as evidenced by thermo-programmed desorption (see relevant mass spectrum in Figure S2).

To establish the mechanism of photolysis on the MAS surface for the MAS/NH<sub>3</sub> system, we applied the method developed earlier<sup>6</sup> based on the effect of a surface photo-reaction on the photostimulated defect formation. This method allows us to distinguish whether or not the photostimulated surface reaction is catalytic. If not catalytic, then what might be the major pathway—interaction with electrons or holes? The latter can be established from a comparison of photocoloration kinetics *in vacuo* and during well-established noncatalytic processes of photostimulated adsorption of oxygen, which represents a reduction due to interaction of O<sub>2</sub> with surface-active electron states only, and photoadsorption of hydrogen that represents an oxidation caused by interaction of H<sub>2</sub> with surface-active hole states. These represent two extreme cases of surface photoreactions.

To demonstrate the existence of these hole states in MAS, we sought evidence of their existence by diffuse reflectance spectroscopy (DRS). UV irradiation of MAS *in vacuo* led to the photogenerated V-type color centers resulting in the appearance of the absorption in a wide spectral range (250–900 nm) in the DRS spectrum illustrated in Figure 2.

Introducing ammonia onto a prephotoactivated surface led to the partial decay of the 360 nm absorption band corresponding to surface V-type centers (Figure 2) because of the interaction of surface V-type centers with ammonia molecules in a manner similar to the effect of hydrogen photoadsorption.<sup>8</sup> Accordingly, a possible reaction pathway is interaction of gaseous ammonia with these surface V-type hole centers formed during the photoactivation of the spinel surface *in vacuo*. In this case, hydrazine was detected (see Figure S2) by thermo-programmed desorption as a surface reaction product formed after adsorption of ammonia on V-type centers.

The resulting kinetics of photocoloration of MAS at 360 nm corresponding to light absorption by V-type hole color centers during the photolysis of ammonia on the surface of MAS are illustrated in Figure 3. The kinetic course of formation of V-type centers in MAS during UV irradiation *in vacuo*, and during the photostimulated adsorptions of oxygen and hydrogen are also shown for comparison. It is evident that the kinetics of



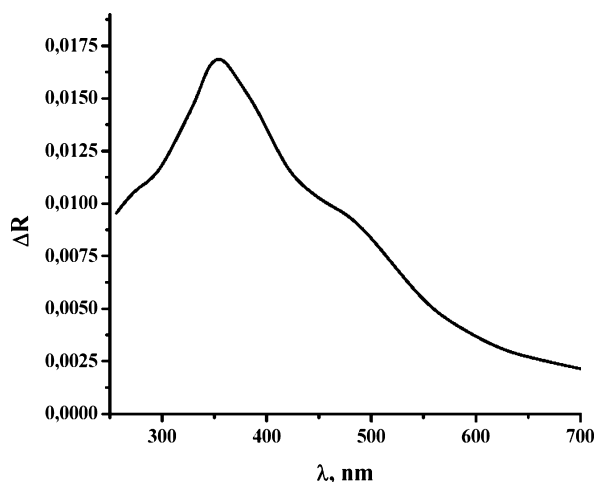


**Figure 2.** Difference diffuse reflectance spectrum of surface V-type hole centers that interact with gaseous ammonia.

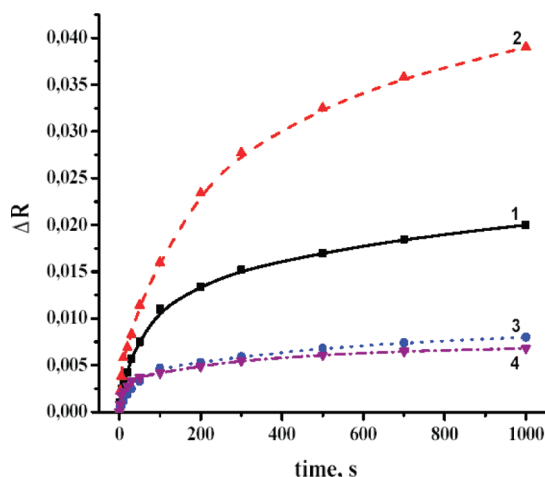


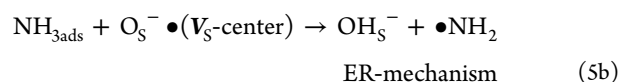
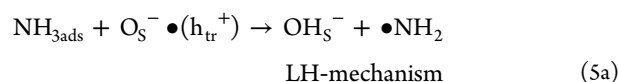
**Figure 3.** Kinetics of photogeneration of V-type hole color centers ( $\lambda = 360$  nm) during the UV irradiation of MAS *in vacuo* (curve 1), and in the presence of oxygen (curve 2), hydrogen (curve 3), and preadsorbed ammonia (curve 4).

photocoloration of MAS during the photolysis of ammonia (curve 4) differ strongly from the photocoloration kinetics *in vacuo* (curve 1) and in the presence of oxygen (curve 2). However, they are in accord with the kinetics of formation of V-type centers observed during the photostimulated adsorption of hydrogen (curve 3). This infers that the mechanism of ammonia photolysis parallels the mechanism of hydrogen photoadsorption. As such, ammonia photolysis is caused by the interaction of adsorbed  $\text{NH}_3$  molecules with surface-active hole states.

A flash of light corresponding to the PhICL effect was observed during the adsorption of ammonia on the photo-activated MAS; the emitted light monitored at 520 nm decayed within a few seconds (see Figure S3) indicating the presence of secondary radical-induced surface processes. Recall that the PhICL effect is typical of interactions of hydrogen-containing molecules with surface-active hole centers. Under our experimental conditions, we were unable to monitor the wavelength-dependent emission spectrum of this MAS/ $\text{NH}_3$  system. However, we hasten to note that, since the emission spectrum for the hydrogen induced PhICL effect reported earlier by Emeline and Ryabchuk<sup>8</sup> coincides with the

photostimulated and thermostimulated luminescence spectra of MAS, it is not unreasonable to suppose that such a correspondence would also apply to the MAS system whose photostimulated and thermostimulated luminescence spectra also coincide with maxima at ca. 520 nm. Thus, the wavelength 520 nm was chosen to record the decay of the PhICL effect reported in Figure S3 (see Supporting Information).

Regardless of the type of ammonia photolysis, whether occurring through a Langmuir–Hinshelwood type mechanism (photolysis of preadsorbed ammonia molecules) or by the Eley–Rideal mechanism (interaction of gaseous ammonia molecules with photogenerated surface-active centers), the first step of the process is the interaction of ammonia with surface-localized hole states (reactions 5a and 5b; note that the surface-localized hole state may be designated as  $\text{O}_s^- \bullet$  or as a surface-trapped hole,  $h_{tr}^+$ , or as a surface V-type color center,  $V_s$ )



Formed during this first step, the  $\bullet \text{NH}_2$  radicals recombine with each other to produce hydrazine as an intermediate reaction product (reaction 6)



Moreover, the binding energy released during the radical recombination process caused additional excitation of the MAS leading to the manifestation of the PhICL effect (Figure 3).

Continued UV irradiation of MAS resulted in the loss of hydrogen atoms by hydrazine ultimately yielding molecular nitrogen that evolved into the gas phase (Figure 1). The whole process involves only surface-active hole states as evident from the data on photocoloration (Figure 3). We conclude, therefore, that ammonia photolysis is a noncatalytic process, since the initial state of the  $\text{MgAl}_2\text{O}_4$  spinel is not regenerated as required for a photocatalytic process, as argued earlier by Emeline and co-workers.<sup>6,23</sup>

**3.3. MAS/ $\text{NH}_3$ / $\text{CH}_4$  System.** An obvious question is: what would happen if UV photoactivation occurred in the presence of both adsorbed ammonia and methane? Unfortunately, a mass spectroscopic analysis would not distinguish among the specific reaction products of such interaction because of the strong mass peaks from hydrazine and methane oxidation products in the mass spectra during the thermo-programmed desorption. Accordingly, detection of possible reaction products was done by and achieved through using the FTIR method.

Curves 1 and 2 of Figure 4 present the difference FTIR spectra of spinel in the  $\text{C}\equiv\text{N}$  stretching region 1950–2300  $\text{cm}^{-1}$  subsequent to the reaction of ammonia and methane under UV irradiation for 4 h over the spinel surface. The ratio of reactants  $\text{NH}_3/\text{CH}_4$  used for these two cases was different: 1:4 (spectrum 1) and 1:10 (spectrum 2). A band at 2208  $\text{cm}^{-1}$  is observed in both spectra. An additional band at 2111  $\text{cm}^{-1}$  appears in spectrum 1. These bands belong to vibrations of the reaction products. Note that spectra of such reaction products were observed neither for the photostimulated adsorption of methane nor for ammonia photolysis.

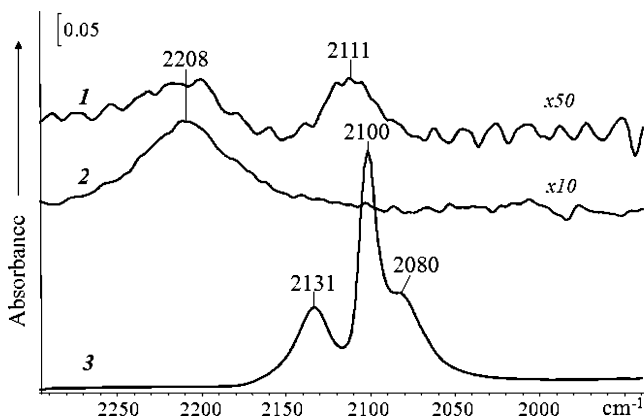


**Figure 4.** FTIR spectra in the  $\text{C}\equiv\text{N}$  stretch region after 4 h of UV irradiation; spectra **1** and **2** were recorded after the reaction of adsorbed  $\text{NH}_3$  with  $\text{CH}_4$  on the  $\text{MgAl}_2\text{O}_4$  surface at 300 K; for different reactants ( $\text{NH}_3/\text{CH}_4$ ) ratios 1:4 (for spectrum **1** – multiplied by 50) and 1:10 (spectrum **2** – multiplied by 10); spectrum **3** is the spectrum of HCN adsorbed on the spinel surface at 180 K.

To identify reaction products, we also examined the adsorption of HCN on the  $\text{MgAl}_2\text{O}_4$  surface as well as on  $\text{MgO}$  and  $\gamma\text{-Al}_2\text{O}_3$  surfaces. Spectra of adsorbed HCN on these samples are presented in Figure 4 and Figure 5. Identification of

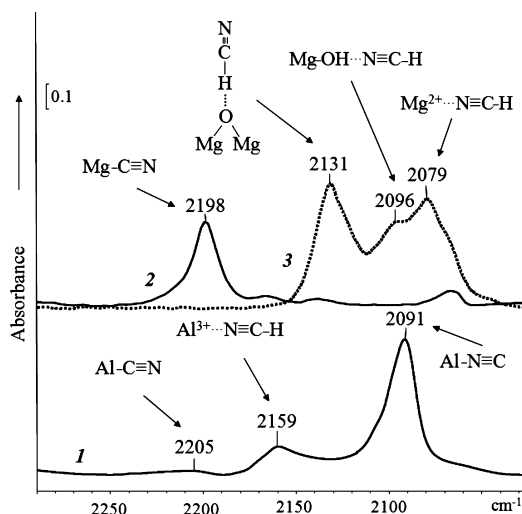


**Figure 5.** FTIR spectra in the  $\text{C}\equiv\text{N}$  stretch region after HCN adsorption: spectrum **1** – on the  $\gamma\text{-Al}_2\text{O}_3$  surface at 300 K; spectrum **2** – on the  $\text{MgO}$  surface at 300 K and after annealing at 550 K; spectrum **3** – on the  $\text{MgO}$  surface at 180 K. Assignments of the various IR bands are also shown.

the numerous bands observed in the spectra was carried out using observations from earlier studies,<sup>24</sup> particularly those by Tsyganenko and co-workers<sup>25,26</sup> and by Kim et al.<sup>27</sup> Figure 5 also displays band assignments of the corresponding surface species.

It seems that, at the lower temperatures, HCN adsorption is nondissociative and occurs on surface OH groups of the metal oxides, on surface cations, and on coordinately unsaturated surface oxygen atoms. The bands at 2198 and 2205  $\text{cm}^{-1}$  assigned to  $\text{CN}^-$  ions start to grow in the spectra at approximately 300 K. The spectrum of HCN adsorbed on the spinel surface is similar to that on the  $\text{MgO}$  surface (spectrum **3**, Figure 4). It should be mentioned that there was

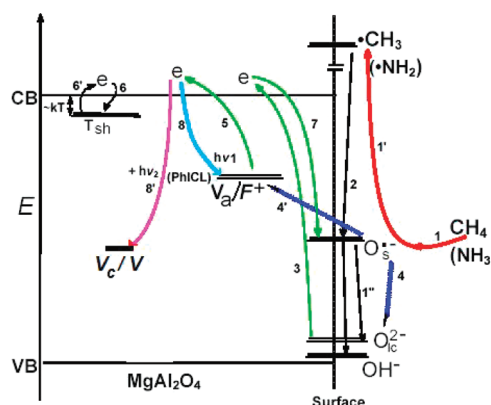
no formation of the  $\text{CN}^-$  ion during the molecular adsorption of HCN on MAS. Therefore, the band at 2208  $\text{cm}^{-1}$  in the spectra of the photoreaction products is assigned to the  $\text{Al}-\text{C}\equiv\text{N}$  and/or to  $\text{Mg}-\text{C}\equiv\text{N}$  surface species. The infrared band at 2111  $\text{cm}^{-1}$ , observed in spectrum **1** of Figure 4, probably belongs to the  $\text{Al}-\text{N}\equiv\text{C}$  surface compound. Formation of the latter may depend on the reactants ratio and, therefore, on the occupation of Lewis acid sites, e.g., surface Al cations.

Thus, interaction of adsorbed ammonia with methane on a UV-activated surface of MAS results in the formation of heteroatomic chemical bonds. It is reasonable to assume that such heteroatomic chemical bonds are formed from the interaction of  $\bullet\text{CH}_3$  and  $\bullet\text{NH}_2$  radicals produced in the first steps of the interaction of methane and ammonia with surface-active hole states, respectively, followed by loss of the remaining hydrogen atoms to form  $\text{CN}_s^-$  species (reaction 7):



Scheme 1 summarizes some of the photophysical events that might occur initially on the photoactivated spinel on

**Scheme 1. Illustration of Possible Events Occurring Whenever a Gas Such As Methane or Ammonia Comes into Contact with a Surface-Active Hole State (Designated as  $\text{O}_s^-\bullet$ )<sup>a</sup>**



<sup>a</sup> $V_a$  denotes an anion vacancy, whereas  $F^+$  designates an  $F$  center with one trapped electron;  $T_{sh}$  denotes a shallow trap for electrons. Note that steps 1, 1' are analogous to reactions 5a and 5b—see text. Also note that the positions of the various levels are rather arbitrary and have no quantitative meaning.

introducing methane and/or ammonia to produce the methyl and amine radical species (steps 1, 1'), respectively, and ultimately through other steps give rise to the PhICL effect via reactions 8 and 9 analogous, respectively, to step 8 and step 8':



Step 2 is related to reaction 3 whereby the surface complex  $\{\text{CH}_3\text{O}\}_s^-$  is formed plus a free electron (not shown). Steps 3 and 5 refer to a possible ionization of a trapped electron in the  $F^+$  color center and from  $\text{O}_{LC}^{2-}$  at energies much greater than the thermal energy  $kT$  due to either energy transfer or photoexcitation by PhICL emission, while steps 4, 4' represent the energy transfer from the surface to the bulk defect and low-coordinated surface states. Step 7 denotes the recombination of a free electron with a surface-trapped hole, whereas steps 6 and

6' correspond, respectively, to the trapping and thermal detrapping of an electron in a shallow trap.

#### 4. CONCLUDING REMARKS

Interaction of hydrogen-bearing molecules, such as methane and ammonia, with photogenerated surface-active hole states produced on the UV-irradiated ( $\text{MgAl}_2\text{O}_4$ ) spinel surface leads to formation of radical species, which on recombination results in the production of molecules more complex than the initial reagent molecules, including heteroatomic species. The latter observation may be relevant to discussions regarding the formation of heteroatomic organic molecules in nature, particularly on the issue of prebiotic stages of the origin of life taking into consideration the possible heterogenic photo-stimulated reactions of gases (e.g., methane and ammonia) on the surface of dust particles in interstellar space and on primitive earth on minerals consisting of complex metal oxides, such as spinel (MAS), during Earth's formation in the period 4.5–3.8 billion years ago.<sup>13</sup>

#### ■ ASSOCIATED CONTENT

##### Supporting Information

Additional figures. This material is available free of charge via the Internet at <http://pubs.acs.org>.

#### ■ AUTHOR INFORMATION

##### Corresponding Author

\*E-mail: [alexei.emeline@spbu.ru](mailto:alexei.emeline@spbu.ru) (A.V.E.) and [nick.serpone@unipv.it](mailto:nick.serpone@unipv.it) or [nickserpone@yahoo.ca](mailto:nickserpone@yahoo.ca) (N.S.).

##### Notes

The authors declare no competing financial interest.

#### ■ ACKNOWLEDGMENTS

The authors are thankful to Prof. A. A. Tsyganenko for useful discussions regarding the interpretation of the FTIR spectra of reaction products. One of us (N.S.) is also grateful to Prof. Albini of the University of Pavia for his kind hospitality in his laboratory over several winter semesters since 2002.

#### ■ REFERENCES

- (1) Solonitsyn, Yu.P.; Kuz'min, G. N.; Shurygin, A. L.; Yurkin, V. M. Quantum Yield of photoadsorption, photo- and X-ray induced adsorption capacity of titanium dioxide with relation to hydrogen and methane. *Kinet. Kataliz* **1976**, *7*, 1267–1372.
- (2) Volodin, A. M.; Cherkasin, A. E. ESR Spectrum of methyl radicals on ZnO Surface. *React. Kinet. Catal. Lett.* **1981**, *18*, 243–246.
- (3) Che, M.; Tench, A. J. Characterization and Reactivity of Mononuclear Oxygen Species on Oxide Surfaces. *Adv. Catal.* **1982**, *31*, 77–133.
- (4) Kaliaguine, S. L.; Shelimov, B. N.; Kazansky, V. B. Reactions of methane and ethane with hole centers  $\text{O}^-$  on  $\text{TiO}_2$ . *J. Catal.* **1978**, *55*, 384–393.
- (5) Kuz'min, G. N.; Knat'ko, M. V.; Kurganov, S. V. Light and X-rays induced chemistry of methane on  $\text{TiO}_2$ . *React. Kinet. Catal. Lett.* **1983**, *3*, 313–318.
- (6) Emeline, A. V.; Kataeva, G. V.; Panasuk, A. V.; Ryabchuk, V. K.; Sheremetyeva, N.; Serpone, N. Effect of surface photoreactions on the photocoloration of a wide band gap metal oxide: probing whether surface reactions are photocatalytic. *J. Phys. Chem. B* **2005**, *109*, 5175–5185.
- (7) Andreev, N. S.; Kotelnikov, V. A. Photoinduced adsorboluminescence on aluminum oxide. *Kinet. Kataliz* **1974**, *15*, 1612–1613.
- (8) Emeline, A. V.; Ryabchuk, V. K. A Spectral Study of the Centers of Photosorption of Oxygen and Hydrogen on Dispersed  $\text{MgAl}_2\text{O}_4$

Spinel. *Z. Fiz. Khim* **1998**, *72*, 512–516; *Russ. J. Phys. Chem.* **1998**, *72*, 432–435.

(9) Emeline, A. V.; Polikhova, S.; Andreev, N. S.; Ryabchuk, V. K.; Serpone, N. Photoinduced Processes in Heterogeneous Gas-Solid Systems. Temperature Dependence (100–600 K) and Modeling of a Surface Chemical Reaction on Zirconia that Triggers Photophysical Events in the Solid. *J. Phys. Chem. B* **2002**, *106*, 5956–5966.

(10) Andreev, N. S.; Emeline, A. V.; Polikhova, S. V.; Ryabchuk, V. K.; Serpone, N. Photo-induced Adsorption of Hydrogen and Methane on  $\gamma$ -Alumina. The PhICL Effect. *Langmuir* **2004**, *20*, 129–135.

(11) Zamaraev, K. I.; Khramov, M. I.; Parmon, V. N. Possible impact of heterogeneous photocatalysis on the global chemistry of the Earth's Atmosphere. *Catal. Rev. — Sci. Eng.* **1994**, *36*, 617–644.

(12) Parmon, V. N.; Zakharenko, V. S. Photocatalysis and photosorption in the Earth's Atmosphere. *CatTech.* **2001**, *5*, 96–108.

(13) Emeline, A. V.; Otroshenko, V. A.; Ryabchuk, V. K.; Serpone, N. Abiogenesis and Photostimulated Heterogeneous Reactions in Interstellar Media and on Primitive Earth. *J. Photochem. Photobiol., C: Rev.* **2003**, *3*, 203–224.

(14) Woosley, J. D.; Wood, C. Photoelectric effects in magnesium aluminum spinel. *Phys. Rev. B* **1980**, *22*, 1065–1072.

(15) Savhina, T. I.; Merillo, I. A. Photon multiplication in single and double metal oxides. *Trudi Inst-ta Fiziki AN ESSR*, Luschik, Ch. B., Ed.; Tartu, **1979**, *49*, 3–56.

(16) Penkalia, T. Crystal Chemistry Outlines. Leningrad. *Khimia* **1974**, 495.

(17) Cain, L. S.; Pogatshnik, G. I.; Chen, Y. Optical transitions in neutron-irradiated  $\text{MgAl}_2\text{O}_4$  spinel crystals. *Phys. Rev. B* **1988**, *37*, 2645–2652.

(18) White, G. S.; Jones, R. V.; Crawford, J. H., Jr. Optical spectra of  $\text{MgAl}_2\text{O}_4$  exposed to ionizing radiation. *J. Appl. Phys.* **1982**, *53*, 265–270.

(19) Emeline, A. V.; Ryabchuk, V. K. Photostimulated Adsorption of Oxygen and Hydrogen on Dispersed  $\text{MgAl}_2\text{O}_4$  Spinel. *Z. Fiz. Khim.* **1997**, *71*, 2078–2081; *Russ. J. Phys. Chem.* **1997**, *71*, 1881–1884.

(20) Basov, L. L.; Kuz'min, G. N.; Prudnikov, I. M.; Solonitsyn, Yu.P. Photoadsorption processes on metal oxides, *Uspekhi Fotoniiki (Advances in Photonics)*, Vilesov, F. I., Ed.; Leningrad State University, **1977**, *6*, 82–120.

(21) Kurganov, S. V.; Artem'ev, Yu.M. Photoadsorption capacity of silica modified with titanium oxide. *Vestn. Leningr. Univ. Ser. 4: Fiz. Khim.* **1988**, *4* (25), 97–100.

(22) Kasparov, K.Ya.; Terenin, A. N. Optical investigations of activated adsorption. I. Photodecomposition of  $\text{NH}_3$  adsorbed on catalysts. *Acta Physicochim. USSR* **1941**, *15*, 343–365.

(23) Emeline, A. V.; Ryabchuk, V. K.; Serpone, N. Photoreactions occurring on metal-oxide surfaces are not all photocatalytic. Description of criteria and conditions for processes to be photocatalytic. *Catal. Today* **2007**, *122*, 91–100.

(24) Babaeva, M. A.; Bystrov, D. S.; Kovalin, A.Yu.; Tsyganenko, A. A. CO Interaction with the surface of thermally activated CaO and MgO. *J. Catal.* **1990**, *123*, 396–416.

(25) Tsyganenko, A. A.; Storozhev, P.Yu.; Otero Arian, C. IR-Spectroscopic Study of the Binding Isomerism of Adsorbed Molecules. *Kinet. Catal.* **2004**, *45*, 530–540.

(26) Tsyganenko, A. A.; Chizhik, A. M.; Chizhik, A. I. A FTIR search for linkage isomerism of CN ions adsorbed on oxides and zeolites. *Phys. Chem. Chem. Phys.* **2010**, *12*, 6387–6395.

(27) Kim, S.; Sorescu, D. C.; Yates, J. T., Jr. Infrared Spectroscopic Study of the Adsorption of HCN by  $\gamma$ - $\text{Al}_2\text{O}_3$ : Competition with Triethylenediamine for Adsorption Sites. *J. Phys. Chem. C* **2007**, *111*, 5416–5425.